1412–1423 *Nucleic Acids Research, 2018, Vol. 46, No. 3* *Published online 23 November 2017*
doi: 10.1093/nar/gkx1182

Dynamic m^{6}A modification regulates local translation of mRNA in axons

Jun Yu[1,2,†], Mengxian Chen[1,†], Haijiao Huang[1,†], Junda Zhu[1], Huixue Song[3], Jian Zhu[1], Jaewon Park[3,4] and Sheng-Jian Ji[1,5,*]

[1]Department of Biology, Southern University of Science and Technology, Shenzhen, Guangdong 518055, China, [2]SUSTech-HKU Joint PhD Program, Southern University of Science and Technology, Shenzhen, Guangdong 518055, China, [3]Department of Electrical and Electronic Engineering, Southern University of Science and Technology, Shenzhen, Guangdong 518055, China, [4]Department of Biomedical Engineering, Southern University of Science and Technology, Shenzhen, Guangdong 518055, China and [5]Institute of Neuroscience, Southern University of Science and Technology, Shenzhen, Guangdong 518055, China

Received October 11, 2017; Editorial Decision November 09, 2017; Accepted November 13, 2017

ABSTRACT

***N*^{6}-methyladenosine (m^{6}A) is a reversible modification in mRNA and has been shown to regulate processing, translation and decay of mRNA. However, the roles of m^{6}A modification in neuronal development are still not known. Here, we found that the m^{6}A eraser FTO is enriched in axons and can be locally translated. Axon-specific inhibition of FTO by rhein, or compartmentalized siRNA knockdown of *Fto* in axons led to increases of m^{6}A levels. *GAP-43* mRNA is modified by m^{6}A and is a substrate of FTO in axons. Loss-of-function of this non-nuclear pool of FTO resulted in increased m^{6}A modification and decreased local translation of axonal *GAP-43* mRNA, which eventually repressed axon elongation. Mutation of a predicted m^{6}A site in *GAP-43* mRNA eliminated its m^{6}A modification and exempted regulation of its local translation by axonal FTO. This work showed an example of dynamic internal m^{6}A demethylation of non-nuclear localized mRNA by the demethylase FTO. Regulation of m^{6}A modification of axonal mRNA by axonal FTO might be a general mechanism to control their local translation in neuronal development.**

INTRODUCTION

N^6-methyladenosine (m^{6}A) is the most widely distributed internal modification in mRNA (1–3). m^{6}A modification of mRNA is a dynamic and reversible process which occurs in nuclear speckles where the methyltransferases ('writers') and demethylases ('erasers') are concentrated (4). The methyltransferase complex including METTLE3, METTL14 and WTAP mediates m^{6}A methylation (5), whereas Fat mass and obesity-associated protein (FTO) (6) and ALKBH5 (7), two demethylases, catalyze demethylation of m^{6}A. m^{6}A modification has been shown to regulate pluripotency of embryonic stem cells and somatic cell reprogramming (8–11), sex determination (12,13), ultraviolet (UV)-induced DNA damage response (14), spermatogenesis (15), haematopoietic stem and progenitor cell specification (16), T cell homeostasis (17), myeloid differentiation (18), cortical neurogenesis (19) and neural circuitry (20). However, the function of m^{6}A in neural development is still largely unknown. FTO which was originally associated with obesity (21), is the first identified m^{6}A eraser (6). Previous studies on FTO in nervous system have focused on its roles in postnatal and elder brains including postnatal growth, brain volume, memory and adult neurogenesis (22–25). However, whether and how FTO regulates neuronal development such as axon growth remains unclear.

Messenger RNAs can be transported and targeted to different subcellular domains and then translated (26–28). Mammalian neurons are extremely polarized cells and mRNA can be transported and stored in their distal subcellular compartment such as axons (29). With the translational machinery in axons, axonal mRNA can be translated locally in axons in response to external cues (30,31). Local translation in axons provides an ideal and economical mechanism for axons (and their growth cones) to rapidly synthesize new proteins needed (32). Local translation in axons has been shown to regulate axon guidance (33–36), axon growth (37,38), axon injury (39), axon regeneration (40,41), neurodegeneration (42), neuronal survival (43), neuronal specification (44), formation and maintenance of neural circuits (45). However, whether 'writing/erasing' of m^{6}A in mRNA can take place in axons and whether m^{6}A

*To whom correspondence should be addressed. Tel: +86 755 88018498; Fax: +86 755 88018498; Email: jisj@sustc.edu.cn
†These authors contributed equally to the paper as first authors.

mRNA modification can regulate local translation in axons are completely unknown.

Here, we investigated whether m^{6}A mRNA modification can regulate local translation in axons. We found that FTO, the m^{6}A eraser which is widely believed to demethylate m^{6}A in nucleus, is enriched in axons. Surprisingly, we found that *Fto* mRNA exists in axons and can be locally translated. We confirmed that *GAP-43* mRNA is m^{6}A-modified. Our data demonstrated that specific inhibition or knockdown of axonal FTO led to elevation of m^{6}A levels of axonal *GAP-43* mRNA, suppression of local translation of *GAP-43* and blocking of axon elongation. Furthermore, our experiments showed that this inhibition effects could be rescued by mutating m^{6}A site of *GAP-43* mRNA. These findings provide important insight into the functional role of m^{6}A modification in regulating local translation in neural development.

MATERIALS AND METHODS

Neuronal culture

The use of animals and protocols were approved by the Laboratory Animal Welfare and Ethics Committee of Southern University of Science and Technology. All reagents used for neuronal cultures were from Thermo Fisher Scientific (USA) unless otherwise specified. Dorsal root ganglia (DRG) neurons were dissected from E13 C57BL/6 mouse embryos in Leibovitz's L-15 medium and dissociated in TrypLE express enzyme. Dissociated neurons or explants of DRG were plated on acid-washed glass coverslips pre-coated with poly-D-lysine (100 μg/ml, Trevigen) and laminin (3.3 μg/ml, Trevigen), and cultured in Neurobasal medium supplemented with B27 (20 ml/l), GlutaMAX Supplement (2 mM), Penicillin–Streptomycin (100 U/ml, 100 μg/ml), 5-fluoro-2′-deoxyuridine (10 μM, Sigma) and Nerve growth factor (NGF) (50 ng/ml). For bath application of rhein, DRG neurons were plated and cultured for 2 h. Then rhein (Sigma) was added to the medium with final concentration of 50 μM. After 4 h, neurons were either processed for immunostaining or used for axon growth assay by taking phase-contrast images.

Knockdown or overexpression using lentiviral system

The lentiviral knockdown plasmid pLKO.1-eGFP was made from pLKO.1-TRC by replacing $Puro^R$ with *eGFP*. The target sequences of shRNA are as following: *shFto*, 5′-GCATGTCAGACCTTCCTAAAG-3′; *shAlkbh5*, 5′-GCATACGGCCTCAGGACATTA-3′; *shMettl3*, 5′-CGTCAGTATCTTGGGCAAATT-3′; *shMettl14*, 5′-CCTGAGATTGGCAATATAGAA-3′; *shYthdf1*, 5′-GCACACAACCTCTATCTTTGA-3′; *shYthdf2*, 5′-GGACGTTCCCAATAGCCAACT-3′; *shYthdf3*, 5′-GCACCTAAACCAACTTCTTGG-3′; *shLacZ (control)*, 5′-GCATAAACCCGCCACTCATCT-3′. The lentiviral overexpression vector pLVX- IRES-eGFP was made from pLVX-IRES-Hyg by replacing Hyg^R with *eGFP*. The lentiviral particles were generated using a second generation packaging system. In brief, HEK293T cells were transfected with 10 μg shRNA-expressing construct or *Fto*-expressing construct, and 8.9 μg pHR and 1.1 μg pVSVG in Opti-MEM (Thermo Fisher Scientific) containing Lipofectamine 3000 (Thermo Fisher Scientific). Cell culture medium containing virus was collected and filtered 48 h post-transfection and then subjected to ultracentrifugation at 22 000 rpm for 2 h at 22°C. The viral pellet was resuspended in 1% bovine serum albumin (BSA) in phosphate-buffered saline (PBS) and stored at −80°C. Neurons were analyzed by immunofluorescence (IF) 48 h after virus transfection.

Microfluidic chamber assays

The master mold for Poly(dimethylsiloxane) (PDMS) replication was fabricated using a two-layer SU-8™ (MicroChem) photolithography process as described in a previous publication (46). First, a silicon wafer with Al alignment marks was prepared. On a cleaned 3-inch silicon wafer, a thin layer of Al (150 nm) was deposited by an e-beam evaporator (HHV Ltd.) and alignment marks were defined by a conventional photolithography process using a positive photoresist (Rzj-304, Suzhou Ruihong Electronic Chemical Co.) followed by an Al etching (Al etchant Type-A, Transene) and stripping of the photoresist (Remover PG, MicroChem). On the silicon wafer with alignment marks, two layers of SU-8™ with different thicknesses were sequentially patterned. First, a 2.5 μm thick channel layer was patterned with SU-8™ 2002 and a 100 μm thick second layer was patterned on top of the first layer using SU-8™ 2075. Two layers were aligned and exposed to UV using a Karl Suss mask aligner (MA6, SÜSS MicroTec).

Microfluidic chambers were replicated from these master molds by cast molding PDMS pre-polymer (10:1 mixture, Sylgard® 184, Dow Corning) at 80°C for 1 h. After punching reservoirs, both microfluidic chamber and cover glass surfaces were treated with corona discharge (BD-20AC, Electro-Technic Products) for 1 min. Then chambers were immediately assembled onto cover glasses. The devices were coated with poly-D-lysine and laminin subsequently. Dissociated DRG neurons were plated into cell body compartments. Axons will typically grow across the microgrooves to the axonal compartment by DIV2–3 for traditional bipartite chambers (Supplementary Figure S3B), and to the distal axon compartment by DIV3–4 for tripartite chambers (Supplementary Figure S3A).

For assays using severed axons, microfluidic chambers were opened by cutting cell body compartments before assembly. DRG explants were plated next to microgrooves and grown in microfluidic chambers for 2DIV and then the cell bodies were removed by forceps. By examining only severed axons, any possibility that changes of axonal proteins or m^{6}A–mRNAs after treatments are due to contribution by soma is excluded.

Immunostaining

Cultured DRG neurons were rinsed with PBS and then fixed with 4% paraformaldehyde/PBS, pH 7.4. After fixation, the neuronal somas and axons were permeabilized and blocked with PBS/0.1% Triton X-100/1% BSA and then incubated with primary antibodies. Primary antibodies in this study were all well described and widely

used in the field. The dilutions and sources of antibodies are as following: FTO (1:500, Phosphosolutions, 597-FTO), ALKBH5 (1:500, Sigma, HPA007196), METTL3 (1:1000, Proteintech, 15073–1-AP), METTL14 (1:1000, Sigma, HPA038002), YTHDF1 (1:500, Abcam, ab99080), YTHDF2 (1:1000, Proteintech, 24744–1-AP), YTHDF3 (1:500, Abcam, ab103328), m^{6}A (1:1000, Synaptic Systems, 202003), Tau1 (1:1000, Millipore, MAB3420), Tau1 (1:1000, Abcam, ab76128) and GAP-43 (1:1000, Millipore, AB5220). Alexa Fluor-conjugated secondary antibodies (Thermo Fisher Scientific) were used at 1:1000. Fluorescent images were acquired using laser-scanning confocal microscopes (Leica SP8 or Nikon A1R) with LASX or NIS software, respectively. All images for each group in the same experiment were collected with identical settings. Quantification of IF signals in axons was performed using ImageJ software for each condition. Specific fluorescence signals from axons were normalized to axon area defined by Tau1 counterstains.

Axonal RNA RT-PCR

DRG neurons were grown in tripartite microfluidic chambers with two microgroove barriers (200 and 500 μm, respectively; illustrated in Supplementary Figure S3A). The design of the tripartite chambers makes sure that no neuronal soma will be present in the distal axon compartment. TRIzol reagent (Thermo Fisher Scientific) was applied to either soma or distal axon compartment (50 μl per compartment). Lysates from 10 chambers were pooled together and total RNA was extracted following the manufacturer's protocol. After first-strand cDNA was synthesized using SuperScript IV First-Strand cDNA Synthesis System (Thermo Fisher Scientific), polymerase chain reaction (PCR) was performed with specific primers for mouse clones as following:

Fto, 5′-GAAGTGGTGAGGATCCAAGG-3′ and 5′-CTGCCTTCGAAGCTGGACTC-3′;

β-actin, 5′- AGGGAAATCGTGCGTGACAT-3′ and 5′-ACGCAGCTCAGTAACAGTCC-3′; *Nrxn2*, 5′- CAGACCTCATCGCTGACGC-3′ and 5′- AGGCGGTCCATCCGTGTAC-3′; *H1f0*, 5′-AGTATATCAAGAGCCACTACAAGG-3′ and 5′-AATGTATTTACAGAAAACAGGAGG-3′.

Axon growth assay

Bright field images were taken using an inverted microscope (Nikon LS100). Axons were manually traced and measured using Image Pro Plus software. For bath application, rhein (50 μM) were added to wells 2 h after plating cells. Three random fields were imaged before and 4 h after rhein treatment. For axon-specific treatment of rhein, DRG neurons were grown in microfluidic chambers and rhein was applied only to axons after axons grew to the axon compartment. The same axons were imaged and analyzed before and after rhein treatment.

Knockdown using siRNA

The designing and transfection of siRNAs were previously reported (44). The target sequences of siRNA are as following: *siNC* (RNAi negative control), 5′-UUCUCCGAACGUGUCACGUTT-3′; *siFto-1*, 5′-GUCAGACCUUCCUAAAGCUTT-3′; *siFto-2*, 5′-CAGGCACCUUGGAUUAUAUTT-3′; *si5s/rRNA*, 5′-CGUCUGAUCUCGGAAGCUATT-3′; *si5.8s/rRNA*, 5′-GCUACGCCUGUCUGAGCGUTT-3′; *si18s/rRNA*, 5′-GCUCGCUCCUCUCCUACUUTT-3′; *si28s/rRNA*, 5′-GCGCCUAGCAGCCGACUUATT-3′. The knockdown was validated by real-time reverse transcriptase (RT)-PCR with primers: *Fto*, 5′-GGAGAGGAAATCCATAATGAGGTG-3′ and 5′-CGCATTTGTCATGCTCTCCAT-3′; *5s rRNA*, 5′-TCTACGGCCATACCACCCTGAACGC-3′ and 5′- GGTATTCCCAGGCGGTCTC-3′; *5.8s rRNA*, 5′-GGTGGATCACTCGGCTCG-3′ and 5′- CAACCGACGCTCAGACAGG-3′; *18s rRNA*, 5′ CTTTGGTCGCTCGCTCCT-3′ and 5′-AGGGAGCTCACCGGGTTG-3′; *28s rRNA*, 5′-CGAGCTCAGGGAGGACAGAA-3′ and 5′-GCCGCCACAAGCCAGTTAT-3′. Measurement of *GAP-43* mRNA levels after rhein treatment or *siFto* knockdown was performed by real-time PCR with primers: *GAP-43*, 5′-ATTCAGGCTAGCTTCCGTGG-3′ and 5′-GCATCGGTAGTAGCAGAGCC-3′.

siRNA-mediated compartmentalized knockdown of *Fto* mRNA or rRNA in axons were carried out using GeneSilencer siRNA Transfection Reagent (Genlantis) following manufacturer's manual and protocols from previous studies (44,47). Briefly, siRNA was mixed with GeneSilencer Reagent and added directly to dishes (for bath application) or axonal compartment of microfluidic chambers (for compartmentalized knockdown). After 48 h, DRG axons and neurons were analyzed by IF or subjected to axon growth assay.

Anti-m^{6}A immunoprecipitation

Immunoprecipitation (IP) of m^{6}A-modified RNA using a specific m^{6}A antibody (Synaptic Systems, 202003) was carried out following a published protocol (48). Briefly, total RNA (1 μg) was incubated with m^{6}A antibody (16 μg/ml) in 1 × IP buffer (10 mM Tris–HCl, 150 mM NaCl, 0.1% Igepal CA-630, 0.4 U/μl RNasin, 2 mM Ribonucleoside vanadyl complexes) and then Dynabeads Protein G (Thermo) was added. After extensive washing with 1 × IP buffer, m^{6}A-modified RNA was eluted using Elution buffer (1 × IP buffer, supplemented with 2.56 mg/ml m6A 5′monophosphate sodium). Eluted RNA was pelleted and used to synthesize cDNA. Then semi-quantitative RT-PCR was carried out to detect *GAP-43* mRNA levels using primers GAP-43-p1, 5′-ATTCAGGCTAGCTTCCGTGG-3′ and 5′-GCATCGGTAGTAGCAGAGCC-3′; GAP-43-p2, 5′-GAGGGAGATGGCTCTGCTACTA-3′ and 5′-AGCCTCGGGGTCTTCTTTAC-3′.

Constructs and nucleofection

The complete cDNA with 3′ untranslated region (3′ UTR) encoding GAP-43 was obtained by RT-PCR from total RNA of DRG. The predicted m^{6}A site (the A immediately following the stop codon: …TGA'A'…) was mutated to C (…TGA'C'…) by PCR. Either wild-type (WT) or m^{6}A-mutated *GAP-43* cDNA with 3′UTR was

cloned to the vector pCAGGS-IRES-eGFP, generating expression constructs pCAGGS-GAP43^{WT}-IRES-eGFP and pCAGGS-GAP43$^{MT\text{-}m6A}$-IRES-eGFP, respectively. Nucleofection of the constructs was performed using a 4D-Nucleofector System machine (LONZA) and P3 Primary Cell 4D-Nucleofector X Kit (LONZA) following the manufacturer's instructions. Briefly, dissociated DRG neurons were re-suspended in Nucleofector Solution ($5 \times 10^5 - 10 \times 10^5$ cells in 20 μl for each condition). After 1 μg of plasmid was added, the mixture was transferred to a well in the 16-well Nucleocuvette Strips and run program DC-100. Then the cells were transferred from the well and plated to microfluidic chambers for culturing. After axons grew to the axonal compartment, rhein was added specifically to axons. Only GFP$^+$ axons were measured for GAP-43 IF and checked for axon growth rates.

Statistical analysis

No statistical methods were used to pre-determine sample sizes, but our sample sizes were similar to those generally applied in the field. Data distribution was assumed to be normal, but this was not formally tested. Samples were randomly allocated to different groups. Data collection and analysis were not performed in a blinded manner to the conditions of the experiments. No data points were excluded from the analyses. Data are mean ± s.e.m. All experiments were conducted at a minimum of three independent biological replicates in the lab. Graphs and statistical analysis were performed using GraphPad Prism 5 software and SPSS software. A P-value < 0.05 was considered as statistically significant. One-way analysis of variance (ANOVA) with Tukey's post test was employed to the comparison of three or more groups. Unpaired, two-tailed t-test was performed for comparison of changes between two groups.

RESULTS

FTO is enriched in axons and derived from local translation

To explore whether m^{6}A can regulate local translation in axons, we first tested whether m^{6}A writers, erasers and readers are expressed in axons. Embryonic day 13 (E13) DRG were dissected, dissociated and cultured *in vitro*. The expression of m^{6}A writers, erasers and readers were examined by immunostaining of DRG neurons with antibodies which are widely used to specifically detect FTO (49), ALKBH5 (7), METTL3 (6), METTL14 (49), YTHDF1 (50), YTHDF2 (49) and YTHDF3 (50). As shown in Figure 1A and B, in addition to soma (both nucleus and cytoplasm), FTO is also enriched in axons. This is surprising since FTO is traditionally thought to work in nucleus and its substrate is m^{6}A in nuclear RNA (6). The localization of FTO in axons suggests that this non-nuclear pool of FTO might play roles in axons and axonal RNA might be its substrate as well. The expression of other m^{6}A writers, erasers and readers in axons are generally very low compared with FTO (Supplementary Figure S1). The specificity of these antibodies used in IF was further verified by knockdown experiments, in which the IF signals of these m^{6}A writers, erasers and readers were gone or significantly decreased after lentiviral shRNAs against *Fto*, *Mettl3*, *Mettl14*, *Alkbh5*, *Ythdf1*, *Ythdf2* and *Ythdf3* were transfected to DRG neurons (Supplementary Figure S2).

The enrichment of FTO in axons suggests that it might be locally translated. To test this possibility, we first investigated whether *Fto* mRNA is localized in axons or not. For local translation studies in axons, microfluidic chambers are powerful platforms which can realize fluidic isolation of axons from soma (51). We cultured DRG neurons in tripartite microfluidic chambers which were designed to prepare pure axonal materials (44). The design with two barriers of microgrooves ensures that there is no possibility of cell body migration to the distal axon compartment (Supplementary Figure S3A). RT-PCR using axonal and soma RNA showed that *Fto* mRNA was detected in both axons and soma (Figure 1C). Quantitative analysis for expression levels showed that axonal *Fto* mRNA level is higher than *β-actin* and similar as *Nrxn2* mRNA (two positive controls for axonal mRNAs (45,52)) (Figure 1D). The absence of *H1f0* mRNA (a histone transcript restricted to soma which worked as a negative control (53)) from axons confirmed that the axonal material was pure with no neuronal soma incorporation (Figure 1C). The localization of *Fto* mRNA in axons suggests that it might be locally translated. To further test this, we cultured DRG explants in traditional bipartite microfluidic chambers (Supplementary Figure S3B). After axons grew to axonal compartment, DRG culture medium was replaced with NGF-free medium for 4 h. After starvation of NGF, explants were removed to exclude the contribution of axonal FTO by soma and the severed axons were treated with NGF for 1 h. We found that NGF treatment led to increased FTO IF signals in axons, which could be blocked by co-application of cycloheximide, a protein synthesis inhibitor (Figure 1E and F). These data suggest that FTO could be locally translated in axons.

To further confirm that FTO is derived from local translation in axons, we performed compartmentalized knockdown in axons with siRNAs specifically against *Fto* mRNA. First, we tested the knockdown efficiency of siRNAs. Bath application of two siRNAs against FTO (*siFto-1* and *siFto-2*) to cultured DRG neurons showed a significant knockdown (52 ± 2%, 45 ± 4%, respectively) of *Fto* mRNA compared with a negative control siRNA (*siNC*) using real-time PCR (Figure 1G). Then, we did compartmentalized knockdown in axons by applying *siFto-1*, *siFto-2* to axonal compartment in microfluidic chambers. Compared with *siNC*, axon-specific knockdown resulted in 70 and 66% decrease of FTO IF signals in axons by *siFto-1* and *siFto-2*, respectively (Figure 1H and I). Axonal knockdown of *FTO* did not change FTO protein levels in soma (Supplementary Figure S3C and D). These data suggest that axonal FTO is derived from local translation in axons.

Inhibition of FTO increases m^{6}A signals in axons and represses axon elongation

Next, we wanted to explore the functions of axonal FTO in neurons. Rhein, a natural product, was discovered to be a potent small-molecule inhibitor of FTO (54). The good inhibitory activity of the cell-active rhein makes it a powerful tool to study FTO functions in neurons. In normal conditions, m^{6}A levels in axons are much lower than soma in cul-

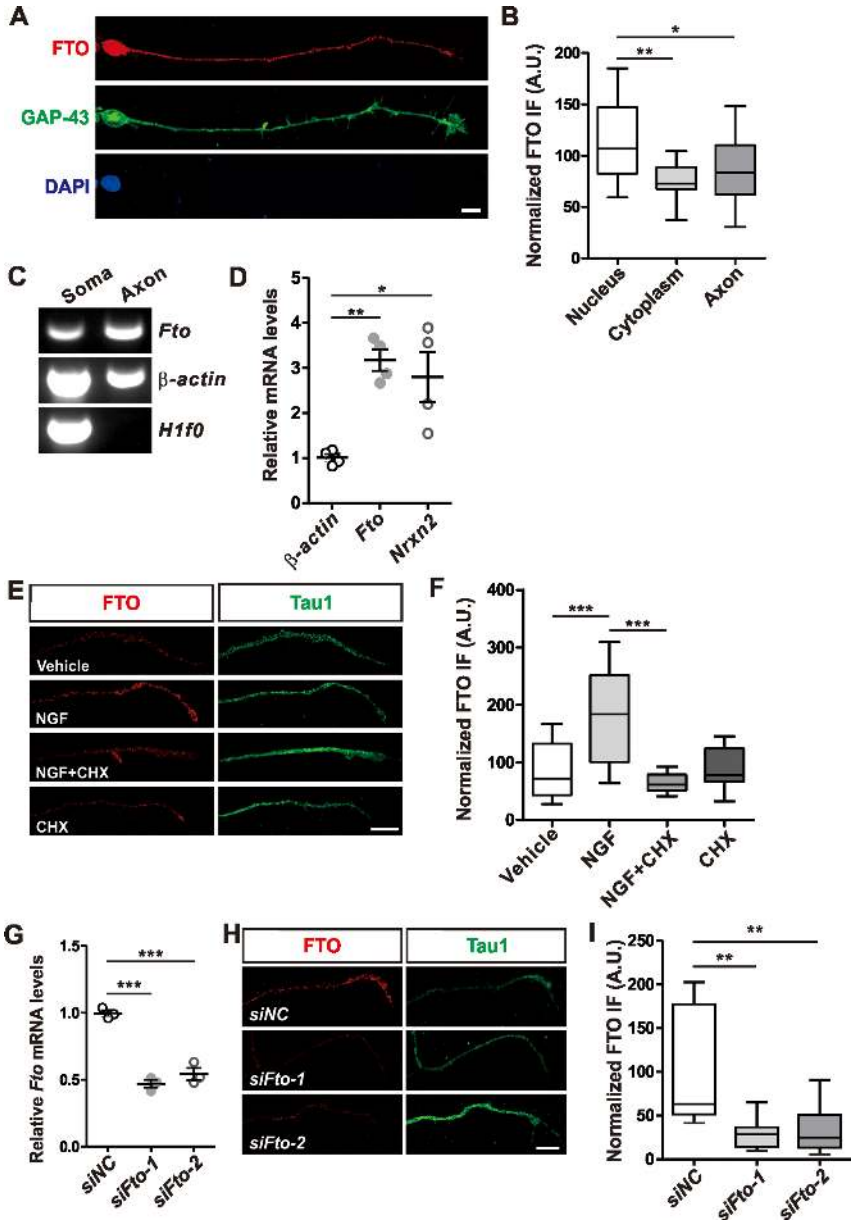

Figure 1. FTO is enriched and locally translated in axons. E13 DRG neurons were cultured and subcellular localization of FTO was examined by immunostaining with a specific antibody. (**A**) Anti-FTO IF showed a strong signal in axons suggesting FTO protein is enriched in axons. GAP-43 is used for counter staining of neurons/axons. (**B**) Quantification of FTO IF signals in nucleus ($n = 18$), cytoplasm ($n = 18$) and axons ($n = 18$). (**C**) *Fto* mRNA was detected in axons. RT-PCR using RNA respectively from distal axon compartment and cell body compartment was carried out. Similar as *β-actin* mRNA which is a positive control for axonal mRNAs, *Fto* mRNA was detected in both axons and soma. The failure to detect *H1f0* mRNA from axons confirmed that the axonal material was pure with no neuronal soma incorporation. (**D**) Axonal quantitaive-PCR (qPCR) analysis showed that axonal *Fto* mRNA has a higher level than *β-actin* mRNA, and is similar as *Nrxn2* mRNA which is another positive control for axonal mRNAs ($n = 4$). (**E**) NGF induces local translation of FTO in axons. DRG explants grown in microfluidic chambers were starved with NGF and then axons were severed from explants to exclude the contribution of axonal FTO by soma. NGF treatment of severed axons resulted in an increase of FTO IF signals in axons, which could be blocked by co-application of cycloheximide (CHX, 10 μM). (**F**) Quantification of results in (E) showing axonal FTO IF intensities (per axonal area defined by Tau1 counter staining) of different treatments (vehicle, $n = 15$ axons; NGF, $n = 16$ axons; NGF + CHX, $n = 10$ axons; CHX, $n = 12$ axons). (**G**) Validation of *siFto*. DRG neurons were cultured and siRNA was transfected by bath application. Compared with a negative control siRNA (*siNC*), two siRNA against *Fto* (*siFto-1*, *siFto-2*) led to significant knockdown of *Fto* mRNA by qRT-PCR ($n = 3$). (**H** and **I**) Compartmentalized knockdown of *Fto* in axons. DRG neurons were grown in microfluidic chambers and siRNA were specifically transfected to axons. Compared with *siNC*, *siFto-1* and *2* led to significant decreases of FTO IF signals (*siNC*, $n = 10$ axons; *siFto-1*, $n = 9$ axons; *siFto-2*, $n = 11$ axons). All data are mean ± s.e.m. Data of IF quantification (B, F and I) are represented as box and whisker plots: 25th–75th percentiles (boxes), minimum and maximum (whiskers) and medians (horizontal lines). For B: nucleus versus cytoplasm, $^{**}P = 0.00207$; nucleus versus axon, $^{*}P = 0.04603$. For F: NGF versus vehicle, $^{***}P = 2.77\text{E-}4$; NGF versus NGF + CHX, $^{***}P = 2.45\text{E-}5$. For I: *siFto-1* versus *siNC*, $^{**}P = 0.00280$; *siFto-2* versus *siNC*, $^{**}P = 0.00318$. qRT-PCR data ($n = 4$ for D and G) are represented as dot plots. For D: *Fto* versus *β-actin*, $^{**}P = 0.00474$; *Nrxn2* versus *β-actin*, $^{*}P = 0.01434$. For G: *siFto-1* versus *siNC*, $^{***}P = 4.39\text{E-}5$; *siFto-2* versus *siNC*, $^{***}P = 1.15\text{E-}4$. All by ANOVA followed by Tukey's multiple comparison test. Each experiment was performed in triplicate (A, C, E, G and H) or quadruplicate (D). Scale bars, 10 μm (A, E and H).

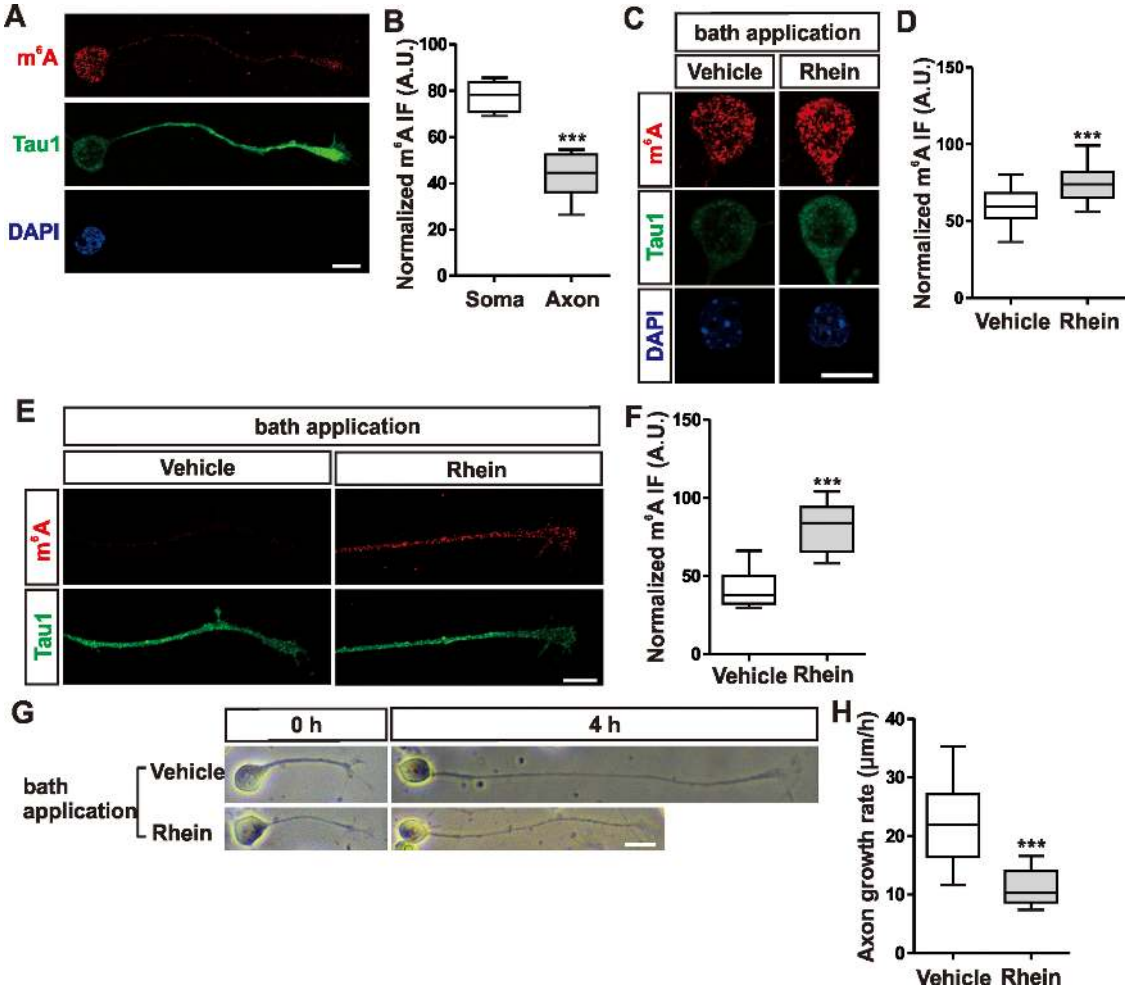

Figure 2. Bath application of rhein increased m^{6}A signals in axons and inhibited axon elongation. (**A** and **B**) m^{6}A signals are much lower in axons than soma. IF was carried out using an m^{6}A-specific antibody and m^{6}A IF signals were quantified in axons and soma, respectively ($n = 9$ neurons). (**C** and **D**) Bath application of rhein in cultured DRG neurons led to a moderate (0.26-fold) increase of m^{6}A signals in soma compared with vehicle treatment (vehicle, $n = 20$ neurons; rhein, $n = 22$ neurons). (**E** and **F**) Bath application of rhein in cultured DRG neurons resulted in a robust increase of m^{6}A signals in axons compared with vehicle treatment (vehicle, $n = 12$ axons; rhein, $n = 12$ axons). This increase (0.95-fold increase) in axons is much bigger than in soma (C and D). (**G** and **H**) Bath application of rhein in cultured DRG neurons inhibited axon elongation by reducing average axon growth rate of 22.17 ± 1.74 μm/h with vehicle treatment to 11.20 ± 0.66 μm/h (vehicle, $n = 16$ neurons; rhein, $n = 20$ neurons). Data are mean ± s.e.m. All data are represented as box and whisker plots: 25th–75th percentiles (boxes), minimum and maximum (whiskers) and medians (horizontal lines). ***$P = 9.88E-8$ (B); ***$P = 6.80E-5$ (D); ***$P = 3.26E-7$ (F); ***$P = 2.60E-7$ (H); by unpaired t-test. Each experiment was performed in triplicate. Scale bars, 10 μm (A, C, E and G).

tured DRG neurons (Figure 2A and B). Bath application of rhein led to a moderate increase (0.26-fold increase compared with vehicle treatment) of m^{6}A in soma (Figure 2C and D). However, a dramatic increase (0.95-fold increase) of m^{6}A signals in axonal RNAs by rhein treatment was observed (Figure 2E and F). The normally low level, and the significant upregulation of m^{6}A levels in axonal RNAs by rhein treatment suggest that axonal RNAs are the preferred substrates of axonal FTO which keeps axonal RNAs in a de-(m^{6}A)methylated state. Knockdown of axonal ribosomal RNAs (rRNA) did not change m^{6}A levels in axons (Supplementary Figure S4A–F), suggesting that m^{6}A IF signals and their changes by rhein treatment were mainly observed in axonal mRNAs. This is consistent with the findings that most modifications of rRNA are buried within the ribosome and are not easily accessible (3). We continued to check the effects of rhein treatment on neuronal development. Four hours treatment of rhein in cultured DRG neurons significantly inhibited axon elongation, with axon growth rate of 22.17 ± 1.74 μm/h for vehicle control reducing to 11.20 ± 0.66 μm/h for rhein treatment (Figure 2G and H). These results support that FTO is required for axon elongation.

Next, we wanted to inhibit FTO specifically in axons. DRG explants were grown in microfluidic chambers and after axons grew to the axonal compartment, explants were removed from axons to exclude any further contribution of m^{6}A modified RNA from soma. Then severed axons were treated with rhein for 2 h. Compared with vehicle treatment, axonal m^{6}A signals showed a significant increase after rhein treatment (Figure 3A and B). These data suggest that FTO in axons is required to regulate de-(m^{6}A)methylation of RNAs in axons. We continued to test whether axon-specific treatment of rhein could inhibit axon elongation. Axon-

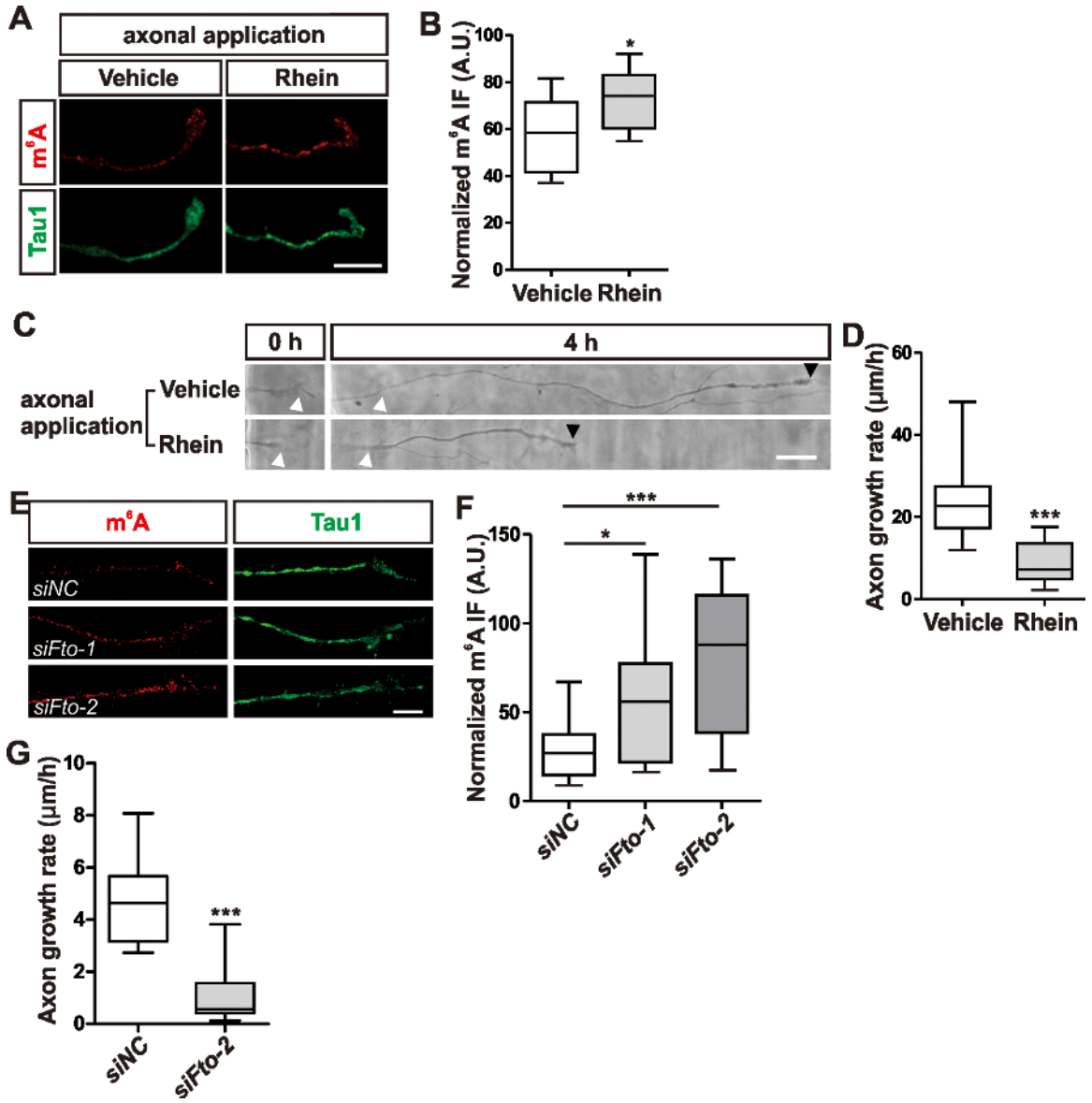

Figure 3. Axon-specific loss-of-function of FTO increased m^{6}A signals in axons and inhibited axon elongation. DRG explants were cultured in microfluidic chambers. After axons grew to the axonal compartment, different experiments were performed. (**A** and **B**) Axonal rhein treatment led to a significant increase of m^{6}A signals in axons (vehicle, $n = 12$ axons; rhein, $n = 10$ axons). Before rhein treatment, axons were severed from explants to prevent any further transport of m^{6}A modified RNA from soma. (**C** and **D**) Rhein treatment of intact axons resulted in a significant reduction of axon growth rate compared with vehicle treatment (vehicle, $n = 16$ axons; rhein, $n = 17$ axons). (**E** and **F**) Compartmentalized *Fto* knockdown in intact axons using two different *siFto* in axons led to significant increase of axonal m^{6}A levels compared with *siNC* (*siNC*, $n = 17$ axons; *siFto-1*, $n = 15$ axons; *siFto-2*, $n = 15$ axons). (**G**) Compartmentalized *Fto* knockdown in intact axons significantly inhibited axon elongation (*siNC*, $n = 8$ axons; *siFto-2*, $n = 10$ axons). Data are mean ± s.e.m. All data are represented as box and whisker plots: 25th–75th percentiles (boxes), minimum and maximum (whiskers) and medians (horizontal lines). For B, D and G: $^*P = 0.0300$ (B); $^{***}P = 2.29\text{E-}6$ (D); $^{***}P = 1.089\text{E-}4$ (G); by unpaired *t*-test. For F: $^*P = 0.038$, $^{***}P = 7.49\text{E-}4$; by one-way ANOVA followed by Tukey's multiple comparison test. Each experiment was performed in triplicate. Scale bars, 10 μm (A, C and E).

specific treatment of rhein in microfluidic chambers for 4 h resulted in a significant decrease of axon elongation rate compared with vehicle control, with axon growth rates of 8.91 ± 1.15 and 23.08 ± 2.22 μm/h, respectively (Figure 3C and D). These results confirmed that activity of axonal FTO was required for axon elongation. To further confirm that the effects on m^{6}A levels and axon elongation by rhein treatment were indeed mediated by FTO, we first prepared axonal-FTO-deficient axons (Figure 1H and I) and then we applied rhein to axons. Under these conditions, rhein treatment could not change m^{6}A levels or axon elongation, suggesting rhein works through FTO in these assays (Supplementary Figure S5A and B).

To confirm more directly that FTO regulates m^{6}A modification and axon elngation in axons, we carried out compartmentalized knockdown of *Fto* in axons using siRNAs (Figure 1H and I). After axon-specific knockdown of *Fto*, axonal m^{6}A levels showed significant increases (Figure 3E and F). Overexpression of FTO led to dramatic decreases of m^{6}A signals both in soma and axons (Supplementary

Figure S5C–J). Axon-specific knockdown of *Fto* also significantly repressed axon elongation (Figure 3G). Together, these results suggest that axonal FTO is required for maintaining axon RNA in a low m^{6}A modification state, and increased axonal m^{6}A levels by inhibition of FTO (with rhein) or knockdown of *Fto* in axons repress axon elongation.

Axonal FTO regulates local translation of *GAP-43* in axons

Local translation of mRNAs targeted to axons and growth cones can regulate neural development. Expression of the growth-associated protein-43 (GAP-43) is required for axon elongation (55). Targeting and local translation of *GAP-43* mRNA in axons regulate axon elongation (37,56,57). However, the mechanisms regulating local translation of *GAP-43* during axon elongation are still not clear. The increased m^{6}A mRNA modification levels and decreased axon elongation by inhibition or knockdown of axonal FTO inspired us to hypothesize that m^{6}A modification regulate axon elongation by controlling local translation of *GAP-43*.

To test this hypothesis, we wanted to know whether FTO can regulate GAP-43 protein levels in axons. Both bath application and axon-specific treatment of rhein led to dramatic decreases of GAP-43 protein level in axons (Figure 4A–D). FTO could control GAP-43 protein level through different mechanisms. First we examined whether FTO could control *GAP-43* mRNA level. Neither rhein treatment nor knockdown of *FTO* could change *GAP-43* mRNA levels (Figure 4E and F). These data suggest that FTO does not regulate transcription or stability of *GAP-43* mRNA. Then we continued to test whether FTO could regulate local translation of *GAP-43* mRNA in axons. Axon-specific co-application of rhein with MG-132, a specific and potent proteasome inhibitor, resulted in a significant decrease of GAP-43 protein in axons compared with MG-132 treatment alone (Figure 4G and H). Since MG-132 blocked protein degradation, any loss of axonal GAP-43 protein by rhein treatment could be only due to inhibition of local translation of *GAP-43* mRNA. Overexpression of FTO led to significant increases of GAP-43 protein levels both in soma and axons (Supplementary Figure S6A–D).Together, these experiments confirm that axonal FTO could regulate local translation of *GAP-43* in axons.

Axonal FTO de-(m^{6}A)methylates *GAP-43* mRNA in axons

Next, we explored the mechanisms by which axonal FTO regulates local translation of *GAP-43* in axons. We hypothesized that axonal FTO regulate local translation of *GAP-43* mRNA by controlling its m^{6}A modification levels in axons. First, we wanted to know whether *GAP-43* mRNA is modified by m^{6}A. Analysis of *GAP-43* mRNA using a mammalian m^{6}A site predictor named SRAMP (*s*equence-based *R*NA *a*denosine *m*ethylation site *p*redictor) (58) demonstrated that *GAP-43* mRNA is modified by m^{6}A and the m^{6}A site is the A immediately after the stop codon (TGA'A'). To verify this, we carried out immunoprecipitation (IP) assay using total RNA extracted from E13 mouse DRG explants and a widely used m^{6}A antibody (1,2,6,8,9,20). Compared with control IgG, m^{6}A antibody pulled down *GAP-43* mRNA which was detected by RT-PCR (Figure 5A). Interestingly, IP experiment done with

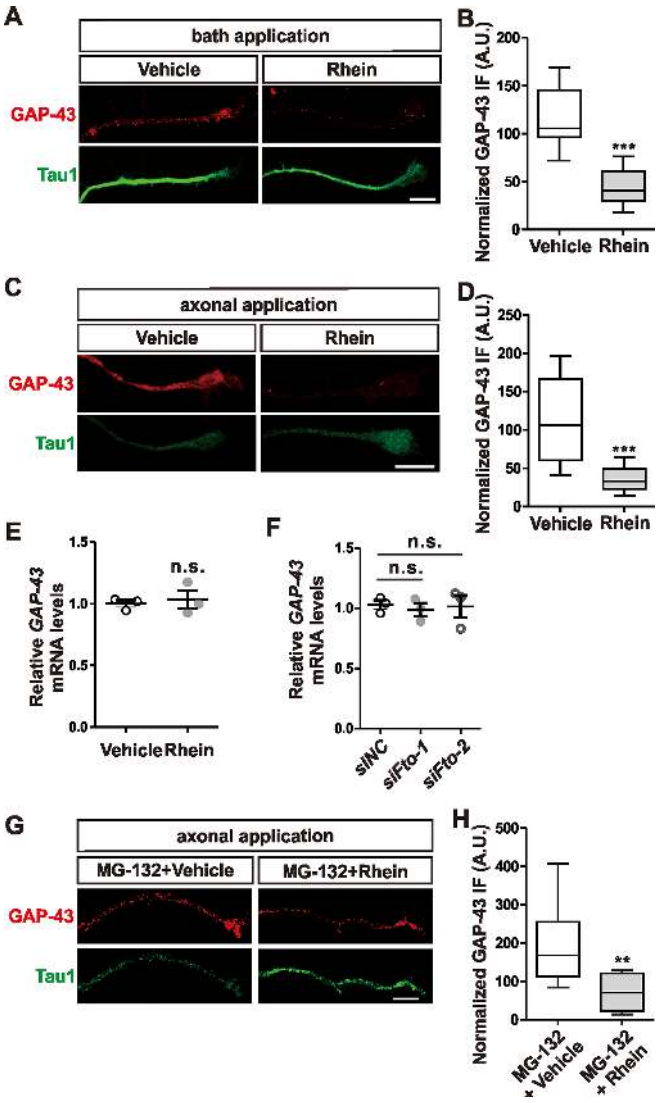

Figure 4. Axonal FTO regulates local translation of *GAP-43* in axons. (**A** and **B**) DRG neurons were cultured *in vitro* and bath application of rhein led to a decrease of GAP-43 IF signals in axons (Vehicle, $n = 15$ axons; Rhein, $n = 14$ axons). (**C** and **D**) Axon-specific treatment of rhein in severed axons resulted in a significant decrease of GAP-43 IF signals in axons (Vehicle, $n = 10$ axons; Rhein, $n = 12$ axons). (**E** and **F**) Loss-of-function of FTO by rhein (E) or *siFto* knockdown (F) did not change *GAP-43* mRNA levels by qRT-PCR ($n = 3$). (**G** and **H**) Co-application of rhein with MG-132 in severed axons led to a significant decrease of GAP-43 IF signals in axons compared with MG-132 treatment alone (MG-132 + Vehicle, $n =$ 11 axons; MG-132 + Rhein, $n = 11$ axons). Data are mean ± s.e.m. IF quantification data (B, D and H) are represented as box and whisker plots: 25th-75th percentiles (boxes), minimum and maximum (whiskers) and medians (horizontal lines). ***$P = 2.76$E-8 (B); ***$P = 0.0002$ (D); **$P =$ 0.0026 (H); by unpaired *t*-test. qRT-PCR data (E and F) are represented as dot plots. n.s., not significant (unpaired *t*-test for E, one-way ANOVA followed by Tukey's multiple comparison test for F). Each experiment was performed in triplicate (C, E, F and G) or quadruplicate (A). Scale bars, 10 μm (A, C and G).

RNA from E13 mouse spinal cord had similar results (Figure 5B). This raises an intriguing possibility that m^{6}A modification of *GAP-43* may be a recurring feature in nervous system. To confirm the m^{6}A site in *GAP-43* mRNA, we generated an expression construct of *GAP-43* with its 3′UTR,

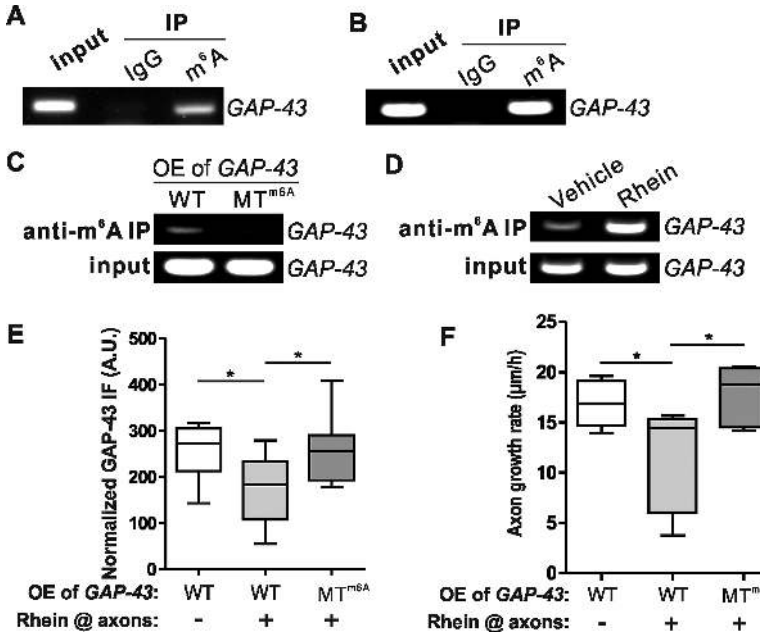

Figure 5. Axonal FTO de-(m^{6}A)methylates *GAP-43* mRNA in axons. (**A** and **B**) Modification of *GAP-43* mRNA by m^{6}A. Total RNA from mouse DRG (A) or spinal cord (B) was immunoprecipitated with a specific m^{6}A antibody or an IgG control. In either of these two tissues, *GAP-43* mRNA was pulled down and detected by RT-PCR. (**C**) Mutation of m^{6}A site eliminated m^{6}A modification in *GAP-43* mRNA. Wild-type ('WT') *GAP-43* or a mutated form which has the predicted m^{6}A site mutated ('MT^{m6A}') were overexpressed in DRG neurons. RNA was purified after rhein treatment for 4 h. After anti-m^{6}A IP, much less *GAP-43* mRNA was detected from 'MT^{m6A}' neurons, compared with 'WT' neurons. (**D**) Rhein treatment led to increase of m^{6}A modification in *GAP-43* mRNA. More *GAP-43* mRNA was pulled down by anti-m^{6}A IP in rhein-treated DRG neurons compared with vehicle control. (**E** and **F**) Mutation of m^{6}A site in *GAP-43* mRNA could rescue inhibition of *GAP-43* local translation and axon elongation by rhein. 'WT' or 'MT^{m6A}' *GAP-43* was overexpressed in DRG neurons and rhein was specifically applied to axons in microfluidic chambers. Axon-specific treatment of rhein in 'WT' *GAP-43*-overexpressing DRG neurons led to significant decreases of GAP-43 protein levels (E) and axon growth rate (F) compared with vehicle control. These decreases were not observed with axonal rhein treatment of 'MT^{m6A}' *GAP-43*-overexpressing DRG neurons (E and F). For E: WT, $n = 15$ axons; WT + Rhein, $n = 10$ axons; MT^{m6A} + Rhein, $n = 8$ axons. For F: WT, $n = 7$ axons; WT + Rhein, $n = 5$ axons; MT^{m6A} + Rhein, $n = 6$ axons. Data are mean ± s.e.m. Data are represented as box and whisker plots: 25th–75th percentiles (boxes), minimum and maximum (whiskers), and medians (horizontal lines). For E: WT versus WT + Rhein, $^*P = 0.01006$; WT + Rhein versus MT^{m6A} + Rhein, $^*P = 0.02977$. For F: WT versus WT + Rhein, $^*P = 0.04229$; WT + Rhein versus MT^{m6A} + Rhein, $^*P = 0.01899$; by one-way ANOVA followed by Tukey's multiple comparison test. Each experiment was performed in triplicate.

in which the predicted m^{6}A site (TGA'A') was mutated to TGA'C'. Overexpression constructs of WT *GAP-43* ('WT') and m^{6}A-mutated *GAP-43* ('MT^{m6A}') were transfected to DRG neurons by nucleofection and total RNAs were extracted respectively after rhein treatment. After IP with m^{6}A antibody, much less *GAP-43* mRNA with m^{6}A site mutated ('MT^{m6A}') was pulled down compared with 'WT' control (Figure 5C; Supplementary Figure S6E). Together, these data suggest that *GAP-43* mRNA is modified by m^{6}A at the A after stop codon.

As experiments shown earlier, axonal FTO keeps axonal RNAs in a de-(m^{6}A)methylated state (Figure 2A, B, E and F). We hypothesized that *GAP-43* mRNA is modified by m^{6}A in soma, and once transported to axons, *GAP-43* mRNA is de-(m^{6}A)methylated by axonal FTO and locally translated to promote axon elongation. This hypothesis is supported by the results that axon-specific loss of function of FTO by rhein treatment inhibited local translation of *GAP-43* (Figure 4C, D, G and H) and axon elongation (Figure 3C and D). To further test this hypothesis, we carried out experiments to examine whether rhein treatment could increase m^{6}A modification levels of *GAP-43* mRNA. Indeed, rhein treatment led to significant increases of m^{6}A levels of *GAP-43* mRNA, which was demonstrated by more *GAP-43* pulled down by m^{6}A antibody after rhein treatment compared with vehicle control (Figure 5D).

Taken together, all the above data support that *GAP-43* mRNA is modified by m^{6}A, and in axons it is de-(m^{6}A)methylated by axonal FTO in order to be locally translated and promote axon elongation.

Mutation of m^{6}A site in *GAP-43* mRNA can rescue inhibition of *GAP-43* local translation and axon elongation by rhein

We next wanted to test whether mutation of m^{6}A site in *GAP-43* mRNA can rescue the inhibition of its local translation by rhein. Overexpression constructs of WT *GAP-43* ('WT') and m^{6}A-mutated *GAP-43* ('MT^{m6A}') were transfected to DRG neurons by nucleofection and axonal GAP-43 protein levels were measured by IF. Axon-specific rhein treatment inhibited axonal GAP-43 protein levels compared with vehicle control with overexpression of WT *GAP-43* (Figure 5E). This is similar with results by measuring endogenous axonal GAP-43 protein levels after rhein treatment in axons (Figure 4C and D). These results suggest that failure to de-(m^{6}A)methylate axonal *GAP-43* mRNA due to rhein treatment, which kept axonal *GAP-43* mRNA in a m^{6}A-modifed state, inhibited local translation of *GAP-43* in

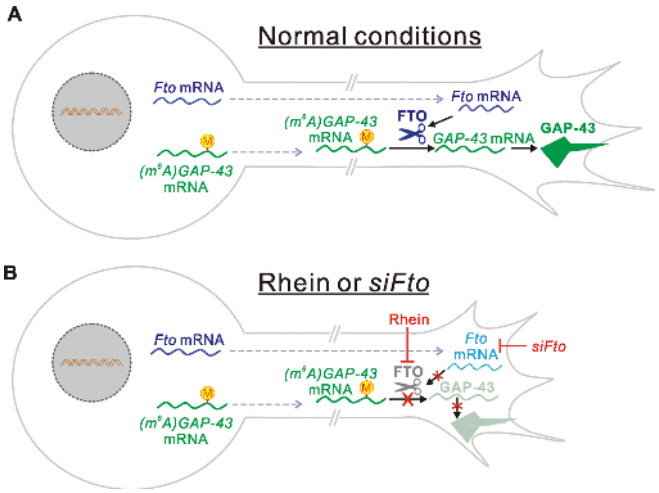

Figure 6. Working model. (**A**) Under normal conditions, *Fto* mRNA is transported to axons and can be locally translated. These axonally derived FTO can de-(m^{6}A)methylate *GAP-43* mRNA. De-(m^{6}A)methylated *GAP-43* mRNA can be locally translated to promote axon elongation. (**B**) Compartmentalized *siFto* knockdown in axons will lead to failure of local translation of *Fto* in axons. Axon-specific treatment of rhein will inhibit FTO functions. Both of these two loss-of-function assays of axonal FTO will result in inhibiting de-(m^{6}A)methylation of *GAP-43* mRNA. Axonal *GAP-43* mRNA with maintained m^{6}A modifications cannot be locally translated, thus inhibiting axon elongation.

axons. However, GAP-43 protein level with overexpression of the m^{6}A-mutated *GAP-43* ('MT^{m6A}') was not subject to rhein inhibition (Figure 5E), because *GAP-43* mRNA was now in a de-(m^{6}A)methylated state and could be locally translated. Similar results were observed with axon growth rate (Figure 5F). These results further support that axonal *GAP-43* mRNA is de-(m^{6}A)methylated by axonal FTO and then locally translated.

DISCUSSION

FTO is traditionally thought to work in nucleus (6). Here we find a novel and unexpected expression and localization of FTO in axons. Another surprising finding is that these non-nuclear FTO is derived from local translation of *Fto* mRNA in axons (illustrated in Figure 6A). Previously it was thought that substrate of FTO is m^{6}A in nuclear RNA (6). Here we find that these axonally derived FTO can de-(m^{6}A)methylate m^{6}A in axonal RNA such as *GAP-43* mRNA, which can then be locally translated in axons to promote axon elongation. Axon-specific loss-of-function of FTO by axonal rhein treatment or compartmentalized siRNA knockdown of *GAP-43* in axons inhibited de-(m^{6}A)methylation, which resulted in maintaining m^{6}A modification of axonal *GAP-43* mRNA (Figure 6B). These *GAP-43* mRNA with maintained m^{6}A modification cannot be locally translated, which results in axon growth inhibition (Figure 6B). Thus FTO has a surprising localization site–axon, previously unknown substrates–axonal RNA and a novel function–regulating local translation in axons.

It is known that m^{6}A modification is reversible and dynamic (59,60). But whether there is a constitutive state of demethylation of m^{6}A and whether this demethylation has a biological role have been under debate. Here we provide an example that dynamic m^{6}A demethylation of axonal mRNA (catalyzed by axonally derived FTO) does occur in axons and has significant roles, e.g. regulating local translation in axons and axon elongation. Our study meets the call for evidence of dynamic cycle of m^{6}A writing/erasing in biological systems (12,61).

Local translation of mRNA in axons plays important roles in neural development including axon guidance, growth and neuronal specification. Local translation can be regulated by various *cis*-elements in axonal mRNAs. For example, some *cis*-acting motifs in axonal mRNAs are required for axonal transport and targeting of mRNA (62,63). miRNA target sequences in axonal mRNA can recruit miRNA such as miR-132, miR-181d and miR-182, and regulate local translation (64–66). There are also other specific motifs in axonal mRNA which can interact with RNA-binding proteins such as ZBP1 and Fus, and regulate local translation (35,67,68). Here, we report a novel regulatory mechanism for local translation, the internal m^{6}A modification of mRNA. Axonal *GAP-43* mRNA which maintains m^{6}A-modification due to loss-of-function of axonal m^{6}A eraser FTO cannot be locally translated. These findings support a model that m^{6}A-modified mRNAs are transported to axons in a silent (not translated) form, and they can be locally translated only when they are de-(m^{6}A)methylated by axonal FTO.

GAP-43 mRNA with maintained m^{6}A-modification fails to be locally translated, which is not due to RNA degradation because *GAP-43* mRNA levels are not changed by rhein or knockdown of FTO. Inhibition of translation (without affecting mRNA stability) by maintained or excess m^{6}A modification is consistent with findings that highly methylated mRNA showed significantly lower translation (69), and too much m^{6}A modification has a negative effect on translation (70).

Our findings are consistent with previous reports that m^{6}A is the target of FTO. A recent study suggests that FTO demethylates m^{6}A$_m$ (N^6, 2′-*O*-dimethyladenosine) in the 5′ cap of mRNA more efficiently than the internal m^{6}A (71). Our results suggest that m^{6}A in axonal *GAP-43* mRNA is indeed the target of axonal FTO. Mutation of the predicted m^{6}A site (TGA'A') in *GAP-43* mRNA eliminates its modification, and exempts regulation of its local translation by axonal FTO. These results, together with our findings that inhibition of FTO has much more pronounced effects on axonal m^{6}A than soma m^{6}A, suggest that the preferred targets of axonal FTO are axonal m^{6}A. Demethylation of m^{6}A$_m$ by FTO reduces the stability of m^{6}A$_m$ mRNAs (71). However, we find that de-(m^{6}A)methylation of axonal *GAP-43* mRNA by axonal FTO does not control its stability since rhein treatment or *siFto* knockdown does not change *GAP-43* mRNA levels. Instead, axonal FTO can regulate local translation of *GAP-43* in axons. Together, our results reveal a novel target (axonal m^{6}A) for an unexpected pool of FTO (axonal FTO). Axonal transcriptome analysis has revealed mRNA encoding many proteins (29). It would be interesting to identify substrate mRNAs of axonal FTO in a transcriptome level. Regulation of local translation of mRNA

by de-(m^6A)methylation in axons might be a general mechanism in nervous system development.

SUPPLEMENTARY DATA

Supplementary Data are available at NAR Online.

ACKNOWLEDGEMENTS

We thank members of the Ji lab for technical support and helpful discussions; Caiguang Yang for reagents; Hongwei Guo and Samie R. Jaffrey for comments and suggestions on the manuscript.

FUNDING

Natural Science Fund of Guangdong Province [2016A030313638 to S.-J.J.]; Basic Research Grant from Science and Technology Innovation Commission of Shenzhen Municipal Government [JCYJ20160331115633182 to S.-J.J.]; China Thousand Talent Program for Young Outstanding Scientists Scholarship (to S.-J.J.); Startup Funds from Southern University of Science and Technology and Peacock Plan of Shenzhen Municipal Government [to S.-J.J. and J.P.]. Funding for open access charge: Startup Funds from Southern University of Science and Technology.

Conflict of interest statement. None declared.

REFERENCES

1. Dominissini,D., Moshitch-Moshkovitz,S., Schwartz,S., Salmon-Divon,M., Ungar,L., Osenberg,S., Cesarkas,K., Jacob-Hirsch,J., Amariglio,N., Kupiec,M. *et al.* (2012) Topology of the human and mouse m6A RNA methylomes revealed by m6A-seq. *Nature*, **485**, 201–206.
2. Meyer,K.D., Saletore,Y., Zumbo,P., Elemento,O., Mason,C.E. and Jaffrey,S.R. (2012) Comprehensive analysis of mRNA methylation reveals enrichment in 3′ UTRs and near stop codons. *Cell*, **149**, 1635–1646.
3. Roundtree,I.A., Evans,M.E., Pan,T. and He,C. (2017) Dynamic RNA modifications in gene expression regulation. *Cell*, **169**, 1187–1200.
4. Lee,M., Kim,B. and Kim,V.N. (2014) Emerging roles of RNA modification: m(6)A and U-tail. *Cell*, **158**, 980–987.
5. Liu,J., Yue,Y., Han,D., Wang,X., Fu,Y., Zhang,L., Jia,G., Yu,M., Lu,Z., Deng,X. *et al.* (2014) A METTL3-METTL14 complex mediates mammalian nuclear RNA N6-adenosine methylation. *Nat. Chem. Biol.*, **10**, 93–95.
6. Jia,G., Fu,Y., Zhao,X., Dai,Q., Zheng,G., Yang,Y., Yi,C., Lindahl,T., Pan,T., Yang,Y.G. *et al.* (2011) N6-methyladenosine in nuclear RNA is a major substrate of the obesity-associated FTO. *Nat. Chem. Biol.*, **7**, 885–887.
7. Zheng,G., Dahl,J.A., Niu,Y., Fedorcsak,P., Huang,C.M., Li,C.J., Vagbo,C.B., Shi,Y., Wang,W.L., Song,S.H. *et al.* (2013) ALKBH5 is a mammalian RNA demethylase that impacts RNA metabolism and mouse fertility. *Mol. Cell*, **49**, 18–29.
8. Chen,T., Hao,Y.J., Zhang,Y., Li,M.M., Wang,M., Han,W., Wu,Y., Lv,Y., Hao,J., Wang,L. *et al.* (2015) m(6)A RNA methylation is regulated by microRNAs and promotes reprogramming to pluripotency. *Cell Stem Cell*, **16**, 289–301.
9. Geula,S., Moshitch-Moshkovitz,S., Dominissini,D., Mansour,A.A., Kol,N., Salmon-Divon,M., Hershkovitz,V., Peer,E., Mor,N., Manor,Y.S. *et al.* (2015) m6A mRNA methylation facilitates resolution of naive pluripotency toward differentiation. *Science*, **347**, 1002–1006.
10. Wang,Y., Li,Y., Toth,J.I., Petroski,M.D., Zhang,Z. and Zhao,J.C. (2014) N6-methyladenosine modification destabilizes developmental regulators in embryonic stem cells. *Nat. Cell Biol.*, **16**, 191–198.
11. Aguilo,F., Zhang,F., Sancho,A., Fidalgo,M., Di Cecilia,S., Vashisht,A., Lee,D.F., Chen,C.H., Rengasamy,M., Andino,B. *et al.* (2015) Coordination of m(6)A mRNA methylation and gene transcription by ZFP217 regulates pluripotency and reprogramming. *Cell Stem Cell*, **17**, 689–704.
12. Haussmann,I.U., Bodi,Z., Sanchez-Moran,E., Mongan,N.P., Archer,N., Fray,R.G. and Soller,M. (2016) m6A potentiates Sxl alternative pre-mRNA splicing for robust Drosophila sex determination. *Nature*, **540**, 301–304.
13. Lence,T., Akhtar,J., Bayer,M., Schmid,K., Spindler,L., Ho,C.H., Kreim,N., Andrade-Navarro,M.A., Poeck,B., Helm,M. *et al.* (2016) m6A modulates neuronal functions and sex determination in Drosophila. *Nature*, **540**, 242–247.
14. Xiang,Y., Laurent,B., Hsu,C.-H., Nachtergaele,S., Lu,Z., Sheng,W., Xu,C., Chen,H., Ouyang,J., Wang,S. *et al.* (2017) RNA m6A methylation regulates the ultraviolet-induced DNA damage response. *Nature*, **543**, 573–576.
15. Lin,Z., Hsu,P.J., Xing,X., Fang,J., Lu,Z., Zou,Q., Zhang,K.J., Zhang,X., Zhou,Y., Zhang,T. *et al.* (2017) Mettl3-/Mettl14-mediated mRNA N6-methyladenosine modulates murine spermatogenesis. *Cell Res.*, **27**, 1216–1230.
16. Zhang,C., Chen,Y., Sun,B., Wang,L., Yang,Y., Ma,D., Lv,J., Heng,J., Ding,Y., Xue,Y. *et al.* (2017) m6A modulates haematopoietic stem and progenitor cell specification. *Nature*, **549**, 273–276.
17. Li,H.B., Tong,J., Zhu,S., Batista,P.J., Duffy,E.E., Zhao,J., Bailis,W., Cao,G., Kroehling,L., Chen,Y. *et al.* (2017) m6A mRNA methylation controls T cell homeostasis by targeting the IL-7/STAT5/SOCS pathways. *Nature*, **548**, 338–342.
18. Vu,L.P., Pickering,B.F., Cheng,Y., Zaccara,S., Nguyen,D., Minuesa,G., Chou,T., Chow,A., Saletore,Y., MacKay,M. *et al.* (2017) The N6-methyladenosine (m6A)-forming enzyme METTL3 controls myeloid differentiation of normal hematopoietic and leukemia cells. *Nat. Med.*, **23**, 1369–1376.
19. Yoon,K.J., Ringeling,F.R., Vissers,C., Jacob,F., Pokrass,M., Jimenez-Cyrus,D., Su,Y., Kim,N.S., Zhu,Y., Zheng,L. *et al.* (2017) Temporal control of mammalian cortical neurogenesis by m6A methylation. *Cell*,**171**, 877–889.
20. Hess,M.E., Hess,S., Meyer,K.D., Verhagen,L.A., Koch,L., Bronneke,H.S., Dietrich,M.O., Jordan,S.D., Saletore,Y., Elemento,O. *et al.* (2013) The fat mass and obesity associated gene (Fto) regulates activity of the dopaminergic midbrain circuitry. *Nat. Neurosci.*, **16**, 1042–1048.
21. Fischer,J., Koch,L., Emmerling,C., Vierkotten,J., Peters,T., Bruning,J.C. and Ruther,U. (2009) Inactivation of the Fto gene protects from obesity. *Nature*, **458**, 894–898.
22. Gao,X., Shin,Y.H., Li,M., Wang,F., Tong,Q. and Zhang,P. (2010) The fat mass and obesity associated gene FTO functions in the brain to regulate postnatal growth in mice. *PLoS One*, **5**, e14005.
23. Ho,A.J., Stein,J.L., Hua,X., Lee,S., Hibar,D.P., Leow,A.D., Dinov,I.D., Toga,A.W., Saykin,A.J., Shen,L. *et al.* (2010) A commonly carried allele of the obesity-related FTO gene is associated with reduced brain volume in the healthy elderly. *Proc. Natl. Acad. Sci. U.S.A.*, **107**, 8404–8409.
24. Widagdo,J., Zhao,Q.Y., Kempen,M.J., Tan,M.C., Ratnu,V.S., Wei,W., Leighton,L., Spadaro,P.A., Edson,J., Anggono,V. *et al.* (2016) Experience-dependent accumulation of N6-methyladenosine in the prefrontal cortex is associated with memory processes in mice. *J. Neurosci.*, **36**, 6771–6777.
25. Li,L., Zang,L., Zhang,F., Chen,J., Shen,H., Shu,L., Liang,F., Feng,C., Chen,D., Tao,H. *et al.* (2017) Fat mass and obesity-associated (FTO) protein regulates adult neurogenesis. *Hum. Mol. Genet.*, **26**, 2398–2411.
26. Holt,C.E. and Bullock,S.L. (2009) Subcellular mRNA localization in animal cells and why it matters. *Science*, **326**, 1212–1216.
27. Lecuyer,E., Yoshida,H., Parthasarathy,N., Alm,C., Babak,T., Cerovina,T., Hughes,T.R., Tomancak,P. and Krause,H.M. (2007) Global analysis of mRNA localization reveals a prominent role in organizing cellular architecture and function. *Cell*, **131**, 174–187.
28. Weatheritt,R.J., Gibson,T.J. and Babu,M.M. (2014) Asymmetric mRNA localization contributes to fidelity and sensitivity of spatially localized systems. *Nat. Struct. Mol. Biol.*, **21**, 833–839.
29. Gumy,L.F., Yeo,G.S., Tung,Y.C., Zivraj,K.H., Willis,D., Coppola,G., Lam,B.Y., Twiss,J.L., Holt,C.E. and Fawcett,J.W. (2011)

Transcriptome analysis of embryonic and adult sensory axons reveals changes in mRNA repertoire localization. *RNA*, **17**, 85–98.
30. Job,C. and Eberwine,J. (2001) Localization and translation of mRNA in dendrites and axons. *Nat. Rev. Neurosci.*, **2**, 889–898.
31. Tcherkezian,J., Brittis,P.A., Thomas,F., Roux,P.P. and Flanagan,J.G. (2010) Transmembrane receptor DCC associates with protein synthesis machinery and regulates translation. *Cell*, **141**, 632–644.
32. Jung,H., Gkogkas,C.G., Sonenberg,N. and Holt,C.E. (2014) Remote control of gene function by local translation. *Cell*, **157**, 26–40.
33. Campbell,D.S. and Holt,C.E. (2001) Chemotropic responses of retinal growth cones mediated by rapid local protein synthesis and degradation. *Neuron*, **32**, 1013–1026.
34. Leung,K.M., van Horck,F.P., Lin,A.C., Allison,R., Standart,N. and Holt,C.E. (2006) Asymmetrical beta-actin mRNA translation in growth cones mediates attractive turning to netrin-1. *Nat. Neurosci.*, **9**, 1247–1256.
35. Welshhans,K. and Bassell,G.J. (2011) Netrin-1-induced local beta-actin synthesis and growth cone guidance requires zipcode binding protein 1. *J. Neurosci.*, **31**, 9800–9813.
36. Wu,K.Y., Hengst,U., Cox,L.J., Macosko,E.Z., Jeromin,A., Urquhart,E.R. and Jaffrey,S.R. (2005) Local translation of RhoA regulates growth cone collapse. *Nature*, **436**, 1020–1024.
37. Donnelly,C.J., Park,M., Spillane,M., Yoo,S., Pacheco,A., Gomes,C., Vuppalanchi,D., McDonald,M., Kim,H.H., Merianda,T.T. *et al.* (2013) Axonally synthesized beta-actin and GAP-43 proteins support distinct modes of axonal growth. *J. Neurosci.*, **33**, 3311–3322.
38. Hengst,U., Deglincerti,A., Kim,H.J., Jeon,N.L. and Jaffrey,S.R. (2009) Axonal elongation triggered by stimulus-induced local translation of a polarity complex protein. *Nat. Cell Biol.*, **11**, 1024–1030.
39. Ben-Tov Perry,R., Doron-Mandel,E., Iavnilovitch,E., Rishal,I., Dagan,S.Y., Tsoory,M., Coppola,G., McDonald,M.K., Gomes,C., Geschwind,D.H. *et al.* (2012) Subcellular knockout of importin beta1 perturbs axonal retrograde signaling. *Neuron*, **75**, 294–305.
40. Walker,B.A., Ji,S.J. and Jaffrey,S.R. (2012) Intra-axonal translation of RhoA promotes axon growth inhibition by CSPG. *J. Neurosci.*, **32**, 14442–14447.
41. Yan,D., Wu,Z., Chisholm,A.D. and Jin,Y. (2009) The DLK-1 kinase promotes mRNA stability and local translation in C. elegans synapses and axon regeneration. *Cell*, **138**, 1005–1018.
42. Baleriola,J., Walker,C.A., Jean,Y.Y., Crary,J.F., Troy,C.M., Nagy,P.L. and Hengst,U. (2014) Axonally synthesized ATF4 transmits a neurodegenerative signal across brain regions. *Cell*, **158**, 1159–1172.
43. Cox,L.J., Hengst,U., Gurskaya,N.G., Lukyanov,K.A. and Jaffrey,S.R. (2008) Intra-axonal translation and retrograde trafficking of CREB promotes neuronal survival. *Nat. Cell Biol.*, **10**, 149–159.
44. Ji,S.J. and Jaffrey,S.R. (2012) Intra-axonal translation of SMAD1/5/8 mediates retrograde regulation of trigeminal ganglia subtype specification. *Neuron*, **74**, 95–107.
45. Shigeoka,T., Jung,H., Jung,J., Turner-Bridger,B., Ohk,J., Lin,J.Q., Amieux,P.S. and Holt,C.E. (2016) Dynamic axonal translation in developing and mature visual circuits. *Cell*, **166**, 181–192.
46. Park,J., Koito,H., Li,J. and Han,A. (2009) Microfluidic compartmentalized co-culture platform for CNS axon myelination research. *Biomed. Microdevices*, **11**, 1145–1153.
47. Hengst,U., Cox,L.J., Macosko,E.Z. and Jaffrey,S.R. (2006) Functional and selective RNA interference in developing axons and growth cones. *J. Neurosci.*, **26**, 5727–5732.
48. Dominissini,D., Moshitch-Moshkovitz,S., Salmon-Divon,M., Amariglio,N. and Rechavi,G. (2013) Transcriptome-wide mapping of N(6)-methyladenosine by m(6)A-seq based on immunocapturing and massively parallel sequencing. *Nat. Protoc.*, **8**, 176–189.
49. Zhou,J., Wan,J., Gao,X., Zhang,X., Jaffrey,S.R. and Qian,S.B. (2015) Dynamic m(6)A mRNA methylation directs translational control of heat shock response. *Nature*, **526**, 591–594.
50. Wang,X., Lu,Z., Gomez,A., Hon,G.C., Yue,Y., Han,D., Fu,Y., Parisien,M., Dai,Q., Jia,G. *et al.* (2014) N6-methyladenosine-dependent regulation of messenger RNA stability. *Nature*, **505**, 117–120.
51. Taylor,A.M., Blurton-Jones,M., Rhee,S.W., Cribbs,D.H., Cotman,C.W. and Jeon,N.L. (2005) A microfluidic culture platform for CNS axonal injury, regeneration and transport. *Nat. Methods*, **2**, 599–605.
52. Olink-Coux,M. and Hollenbeck,P.J. (1996) Localization and active transport of mRNA in axons of sympathetic neurons in culture. *J. Neurosci.*, **16**, 1346–1358.
53. Gracias,N.G., Shirkey-Son,N.J. and Hengst,U. (2014) Local translation of TC10 is required for membrane expansion during axon outgrowth. *Nat. Commun.*, **5**, 3506.
54. Chen,B., Ye,F., Yu,L., Jia,G., Huang,X., Zhang,X., Peng,S., Chen,K., Wang,M., Gong,S. *et al.* (2012) Development of cell-active N6-methyladenosine RNA demethylase FTO inhibitor. *J. Am. Chem. Soc.*, **134**, 17963–17971.
55. Skene,J.H. and Willard,M. (1981) Axonally transported proteins associated with axon growth in rabbit central and peripheral nervous systems. *J. Cell Biol.*, **89**, 96–103.
56. Smith,C.L., Afroz,R., Bassell,G.J., Furneaux,H.M., Perrone-Bizzozero,N.I. and Burry,R.W. (2004) GAP-43 mRNA in growth cones is associated with HuD and ribosomes. *J. Neurobiol.*, **61**, 222–235.
57. Irwin,N., Chao,S., Goritchenko,L., Horiuchi,A., Greengard,P., Nairn,A.C. and Benowitz,L.I. (2002) Nerve growth factor controls GAP-43 mRNA stability via the phosphoprotein ARPP-19. *Proc. Natl. Acad. Sci. U.S.A.*, **99**, 12427–12431.
58. Zhou,Y., Zeng,P., Li,Y.H., Zhang,Z. and Cui,Q. (2016) SRAMP: prediction of mammalian N6-methyladenosine (m6A) sites based on sequence-derived features. *Nucleic Acids Res.*, **44**, e91.
59. Fu,Y., Dominissini,D., Rechavi,G. and He,C. (2014) Gene expression regulation mediated through reversible m(6)A RNA methylation. *Nat. Rev. Genet.*, **15**, 293–306.
60. Cao,G., Li,H.B., Yin,Z. and Flavell,R.A. (2016) Recent advances in dynamic m6A RNA modification. *Open Biol.*, **6**, 160003.
61. Ke,S., Pandya-Jones,A., Saito,Y., Fak,J.J., Vagbo,C.B., Geula,S., Hanna,J.H., Black,D.L., Darnell,J.E. Jr and Darnell,R.B. (2017) m6A mRNA modifications are deposited in nascent pre-mRNA and are not required for splicing but do specify cytoplasmic turnover. *Genes Dev.*, **31**, 990–1006.
62. Rihan,K., Antoine,E., Maurin,T., Bardoni,B., Bordonne,R., Soret,J. and Rage,F. (2017) A new cis-acting motif is required for the axonal SMN-dependent Anxa2 mRNA localization. *RNA*, **23**, 899–909.
63. Andreassi,C., Zimmermann,C., Mitter,R., Fusco,S., De Vita,S., Saiardi,A. and Riccio,A. (2010) An NGF-responsive element targets myo-inositol monophosphatase-1 mRNA to sympathetic neuron axons. *Nat. Neurosci.*, **13**, 291–301.
64. Hancock,M.L., Preitner,N., Quan,J. and Flanagan,J.G. (2014) MicroRNA-132 is enriched in developing axons, locally regulates Rasa1 mRNA, and promotes axon extension. *J. Neurosci.*, **34**, 66–78.
65. Wang,B., Pan,L., Wei,M., Wang,Q., Liu,W.W., Wang,N., Jiang,X.Y., Zhang,X. and Bao,L. (2015) FMRP-mediated axonal delivery of miR-181d regulates axon elongation by locally targeting Map1b and Calm1. *Cell Rep.*, **13**, 2794–2807.
66. Bellon,A., Iyer,A., Bridi,S., Lee,F.C., Ovando-Vazquez,C., Corradi,E., Longhi,S., Roccuzzo,M., Strohbuecker,S., Naik,S. *et al.* (2017) miR-182 regulates Slit2-mediated axon guidance by modulating the local translation of a specific mRNA. *Cell Rep.*, **18**, 1171–1186.
67. Lepelletier,L., Langlois,S.D., Kent,C.B., Welshhans,K., Morin,S., Bassell,G.J., Yam,P.T. and Charron,F. (2017) Sonic Hedgehog guides axons via zipcode binding protein 1-mediated local translation. *J. Neurosci.*, **37**, 1685–1695.
68. Yasuda,K., Zhang,H., Loiselle,D., Haystead,T., Macara,I.G. and Mili,S. (2013) The RNA-binding protein Fus directs translation of localized mRNAs in APC-RNP granules. *J. Cell Biol.*, **203**, 737–746.
69. Qi,S.T., Ma,J.Y., Wang,Z.B., Guo,L., Hou,Y. and Sun,Q.Y. (2016) N6-methyladenosine sequencing highlights the involvement of mRNA methylation in oocyte meiotic maturation and embryo development by regulating translation in Xenopus laevis. *J. Biol. Chem.*, **291**, 23020–23026.
70. Slobodin,B., Han,R., Calderone,V., Vrielink,J.A., Loayza-Puch,F., Elkon,R. and Agami,R. (2017) Transcription impacts the efficiency of mRNA translation via Co-transcriptional N6-adenosine methylation. *Cell*, **169**, 326–337.
71. Mauer,J., Luo,X., Blanjoie,A., Jiao,X., Grozhik,A.V., Patil,D.P., Linder,B., Pickering,B.F., Vasseur,J.J., Chen,Q. *et al.* (2017) Reversible methylation of m6Am in the 5′ cap controls mRNA stability. *Nature*, **541**, 371–375.